

ICEQUAKES ON EKSTRÖM ICE SHELF NEAR ATKA BAY, ANTARCTICA*

By H. VON DER OSTEN-WOLDENBURG

(Institut für Allgemeine und Angewandte Geophysik, Ludwig-Maximilians-Universität München, D-8000 München 2, Federal Republic of Germany)

ABSTRACT. Two seismic arrays recorded in an 11 month field experiment in 1985 the seismicity of Ekström Ice Shelf in the area of an ice rumple and an inlet, situated respectively about 10 km north-west and 7 km north of the German Antarctic station Georg von Neumayer (lat. $70^{\circ}37'S$, long. $08^{\circ}22'W$). Most of the focal depths of the icequakes considered until now are in the range 5–9 m; the ice-rumple area shows extremely high seismic activity. Tensile fracture is the most frequent fault mechanism, although there are a few shear-fracture events. The ice rumple's seismicity provides information on the dynamics of the ice shelf in this area. A comparison of this time-dependent seismicity with tides suggests that most of this seismicity is induced by tides. The most active period of this seismicity starts at the beginning of low tide and ends at low tide. The location of the epicentres of icequakes recorded at that time and the digital recording on tapes of the seismicity without interruption for 396 h shows a jerky vertical movement of the ice shelf in response to tides; this can be interpreted as a kind of "grater effect", especially at the southern ice-rock boundary of the ice rumple.

The seismicity in the inlet is much less and tensile fracture seems to be the only fault mechanism.

INTRODUCTION

The German Antarctic station Georg von Neumayer (GvN) is situated approximately 7 km to the west of Atka Bay on Ekström Ice Shelf, which is 206 m thick (personal communication from H. Engelhardt, 1986) and which has a north-north-east directed annual flow velocity of about 160 m/a (measured by Köhler, adjacent to GvN in 1981; Köhler, 1981). About 10 km to the north-north-west of GvN, the ice shelf, which is about 100 m thick at that point, is in contact with some small islands. This produces ice rumpled which are irregularities in the ice plate with a maximum elevation of about 30 m. The annual flow velocity in this area was found to be between 25 and 50 m/a (Kobarg and Lippmann, 1986). Six geophones, five each for the vertical and one for the vertical and two horizontal components of ground motion, formed the ice-rumple array to record the local seismicity of this area. This array, equipped with Mark L4 geophones (eigenfrequency: 1 Hz), worked very successfully for a period of about 9 months in 1985 and was positioned around the highest ice rumple (Fig. 1) in this area; the location of the three-component recording geophone is marked by "5-7" in this figure. Moreover, it was possible to erect a seismic station on the top of this ice feature ("8" in Figure 1). The frequency-modulated seismic time series was telemetered from each seismic station to GvN, where it was digitally recorded on tape for a period of 30 s after event detection with a sampling rate of 148 values per channel per second. The seismicity was digitally recorded on tape also without interruption for 396 h in August in order to investigate the

correlation between tides and seismicity; earlier observations made it clear that there the local seismicity is dependent on the tides (Kobarg and Lippmann, 1986; Brodscholl, unpublished).

The seismicity of the inlet area was digitally recorded on tape for only a period of 30 s after event detection. This was done because no tidal-dependent seismicity was observed during the first weeks of operating the inlet array. This array (Fig. 2) was positioned around the end of an inlet, which is situated approximately 7 km north of GvN. The five seismic stations were also equipped with Mark L4 1 Hz geophones, which recorded only the vertical component of the ground motion.

THE DATA

More than 70 000 icequakes were recorded on magnetic tape by the two seismic arrays, and just under 1% of them occurred in the inlet area. In pre-processing of the data, the influences of the PCM (pulse-coded modulation) apparatus and of the seismometers were eliminated from the data. Calculation of the coordinates of the foci was done in three steps: (1) a graphical method was used for estimation of preliminary values for the time of origin t_0 and the coordinates of the epicentres; (2) use of the FASTHYPO computer program (iterative calculation of the coordinates); and (3) use of the JOINT HYPOCENTRE DETERMINATION program (calculates up to 500 events in one processing). The results of each step are used as basic values for the calculation procedure in the next step, so it was possible to ascertain typical errors in latitude and longitude of the epicentre coordinates of between 12 and 50 m. The velocity structure which was used in the location programs is given in Table I (after Hoyer, unpublished). Two icequakes, recorded respectively in the ice-rumple and the inlet areas, are shown in Figures 3 and 4. The event shown in Figure 4 is typical of the events in the inlet area. On the other hand, we found a great variety in the signal characteristics (signal duration, etc.) of the events of the ice-rumple area. Only in the ice-rumple area were we able to record icequakes with different polarity for the onset of the P-wave (i.e. compression and dilation). Most of the ice-rumple events begin with an upward motion (a compression) in the vertical movement of the P-wave, regardless of the azimuth between seismic station and epicentre. For the events with epicentres inside the arrays this means tensile fracture; the observed source-radiation pattern for the P-wave requires this kind of mechanism.

On the basis of Brune's (1970) stress-pulse model for the events recorded with respectively upward and downward motion of the first onset in the vertical movement of the P-wave at different seismic stations, the far-field spectra are given by:

$$\Omega_S(\omega) = R_{\theta\phi}(S) \frac{\sigma'_s r_0}{\mu R} F(\epsilon) \frac{1}{\omega^2 + \omega_0^2} \quad (1)$$

* See *Annals of Glaciology*, Vol. 12, 1989, p. 206 for an extended abstract.

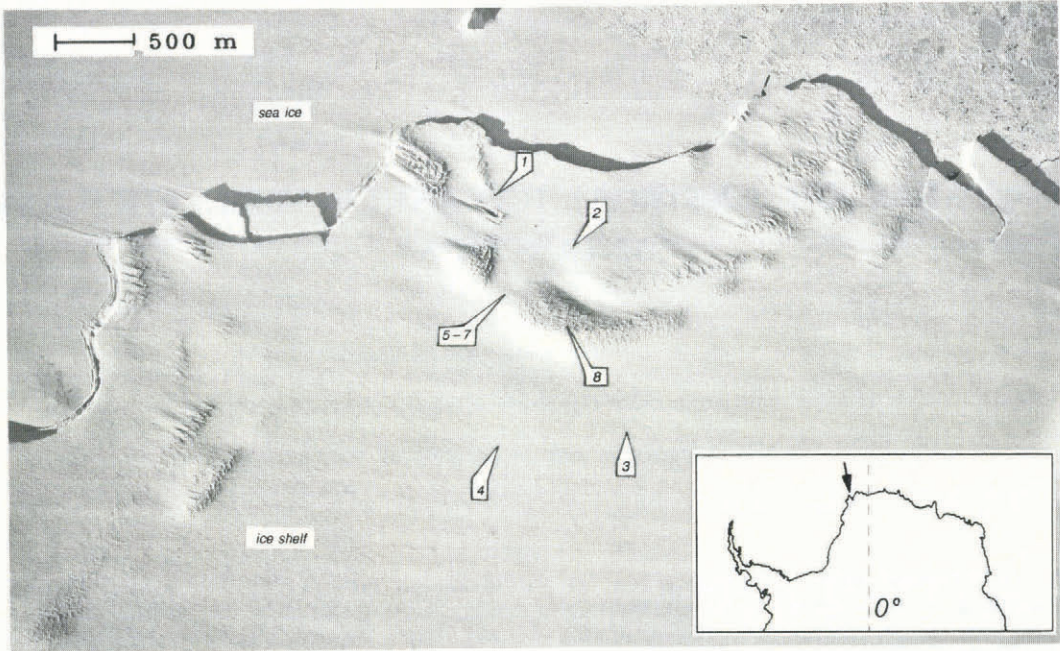
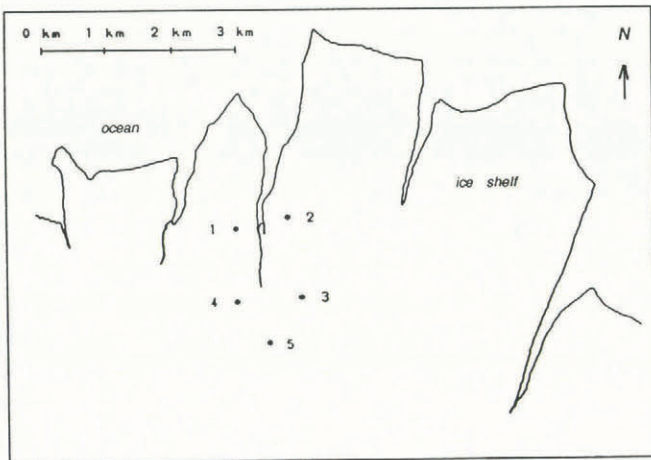


Fig. 1. Ice-rumple area, about 10 km to the north-north-west of Georg von Neumayer. Arrows indicate the sites of the seismometers of this icequake array. This aerophotograph was taken at a height of about 2.6 km by the Institute of Applied Geodesy, Frankfurt/Main, on 3 January 1986. North is at the top.



* geophone site with station number(s)

Fig. 2. Locations of the seismometers of the inlet array which is situated about 7 km north of Georg von Neumayer. North is at the top of this figure. Geophone sites are marked with asterisks.

TABLE I. VELOCITY STRUCTURE USED FOR ICE-QUAKE LOCATIONS

Layer No.	v_p km/s	Top of the layer m
1	0.60	0.000
2	1.00	1.430
3	1.50	3.200
4	2.00	5.000
5	2.20	7.200
6	2.50	12.50
7	3.00	26.40
8	3.50	51.40
9	3.74	80.00

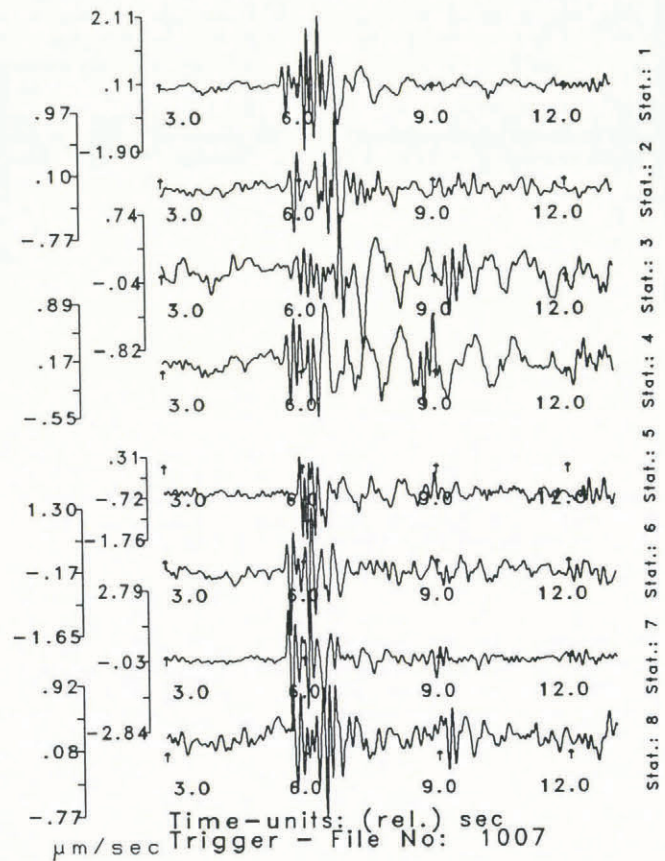


Fig. 3. Icequake recorded by the stations of the ice-rumple array. With the exception of stations 5 and 7, which show the horizontal (respectively north-south and east-west) components of ground motion, all other seismograms show the vertical component.

where R is the distance to the hypocentre, r_0 is the radius of the circular slip zone, σ is the effective stress, $f_0 = \omega_0 / (2\pi)$ is the corner frequency, $F(\epsilon)$ is a factor which takes into consideration incomplete stress-drop across the fault plane, $R_{\theta\phi}$ is the source-radiation pattern of the

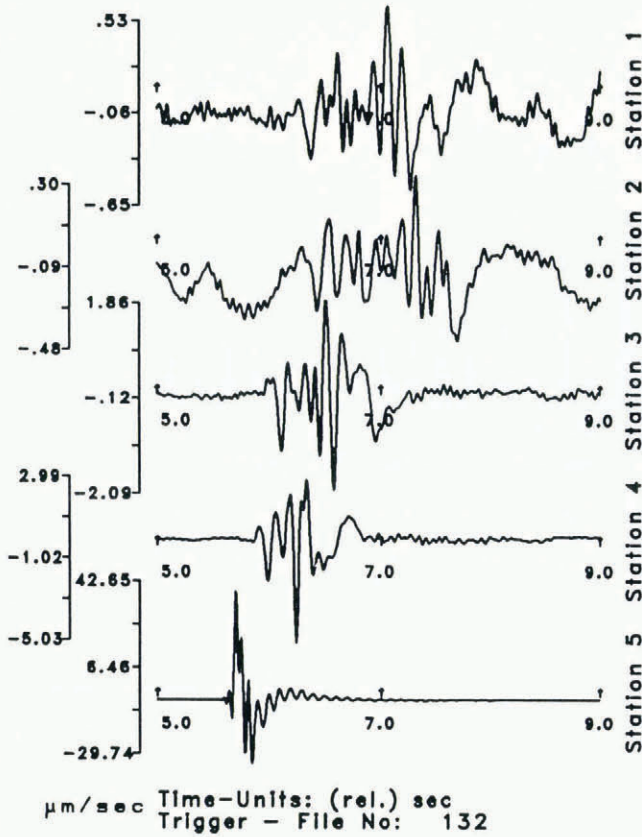


Fig. 4. Typical local event, recorded by the seismometers of the inlet array. The noise at stations 1 and 2 was caused by the high swell on the sea at that time. The epicentre is about 200 m to the south of station 5.

S-wave, μ is the shear modulus, and v_s is the S-wave velocity.

Defining

$$\Omega_{S,0} = \Omega_{S,\omega \rightarrow 0}(\omega) = \frac{R_{\theta\varphi}(S)\sigma v_s r_0 F(\epsilon)}{\mu R \omega_0^2} \quad (2)$$

we can write instead of Equation (1):

$$\Omega_S(f) = \frac{\Omega_{S,0}}{1 + \left(\frac{f}{f_0}\right)^x} \quad (3)$$

For $f \ll f_0$, Equation (3) is nearly independent of the frequency f . This means $\Omega_S(f) \approx \Omega_{S,0}$ which we call the plateau (and which is directly proportional to the seismic moment). For high frequencies, the decay of the spectral values $\Omega_S(f)$, which is caused because of destructive interference of coherent wave trains, is dependent on the exponent x . The frequency at which this decay begins is called the corner frequency f_0 and provides information about other physical parameters of the seismic event. To estimate the plateau $\Omega_{S,0}$, the corner frequency f_0 , and the exponent x , the S-wave spectra have been fitted to Equation (3) (Fig. 5). The x -values of some icequakes are slightly different from $x = 2$, which is obtained from the theory of Brune (Equation (1)).

Using (Brune, 1970)

$$f_0(S) = \frac{2.34 v_s}{2\pi r_0} \quad (4)$$

where v_s is the S-wave velocity ($= 3.74$ km/s), r_0 is the radius of circular fault area, and $f_0(S)$ is the corner frequency of S-wave spectra, we make estimates of the radius of the fault area which are in the range 15–70 m as considered so far.

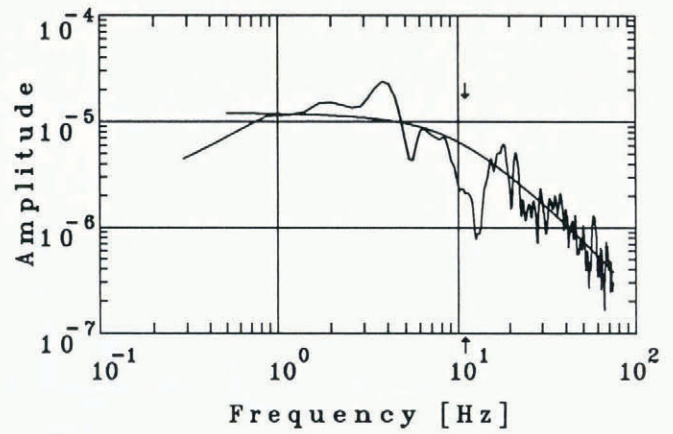


Fig. 5. Spectrum of an integrated S-wave seismogram of an ice-rumple event and the best fit with Equation (3). The corner frequency (marked by arrows) of 11 Hz corresponds to a radius of the circular focal area of about 61 m.

First estimates for the seismic moments are made using (Aki and Richards, 1980)

$$M_0 = 4\pi\rho R v_p^3 \frac{1}{R_{\theta\varphi}(P)} \int_{t_p}^{t_s} u dt \quad (5)$$

where M_0 is the seismic moment, ρ is the density ($= 0.85$ g/cm³), R is the distance between the seismic station and the hypocentre, t_p is the arrival time of the P-wave, t_s is the arrival time of the S-wave, $R_{\theta\varphi}(P)$ is the source-radiation pattern of the P-wave, and u is the real displacement.

For all events, the mean value

$$R_{\theta\varphi}(P) = \frac{2}{\pi} \quad (6)$$

was used. To be able to calculate the integral of the P-impulse of the real displacement (which means that any influence of the apparatus and the seismometers has been excluded), the seismograms (velocity-proportional registrations) had to be integrated. The seismic moments of the icequakes which have been interpreted so far are in the range 10^4 – 10^8 N m.

Provided that the logarithm of the ratio A/T (A : maximum displacement amplitude, T : period) and of the distance to the hypocentre are directly dependent on the magnitude M in a linear way, we have

$$M = a_1 + a_2 \log \frac{A}{T} + a_3 \log R \quad (7)$$

with a_1, a_2, a_3 constants, $[A/T] = \mu\text{m/s}$, $[R] = \text{km}$.

In the literature (e.g. Bath, 1981), the factor a_2 is set to 1. We do the same for reasons of simplification. With $M' = M - a_1$, Equation (7) becomes

$$\log \frac{A}{T} = M' - a_3 \log R. \quad (8)$$

The regression leads to

$$a_3 = 1.989 \pm 0.32 \quad (9)$$

and

$$M = a_1 + \log \frac{A}{T} + 1.989 \log R. \quad (10)$$

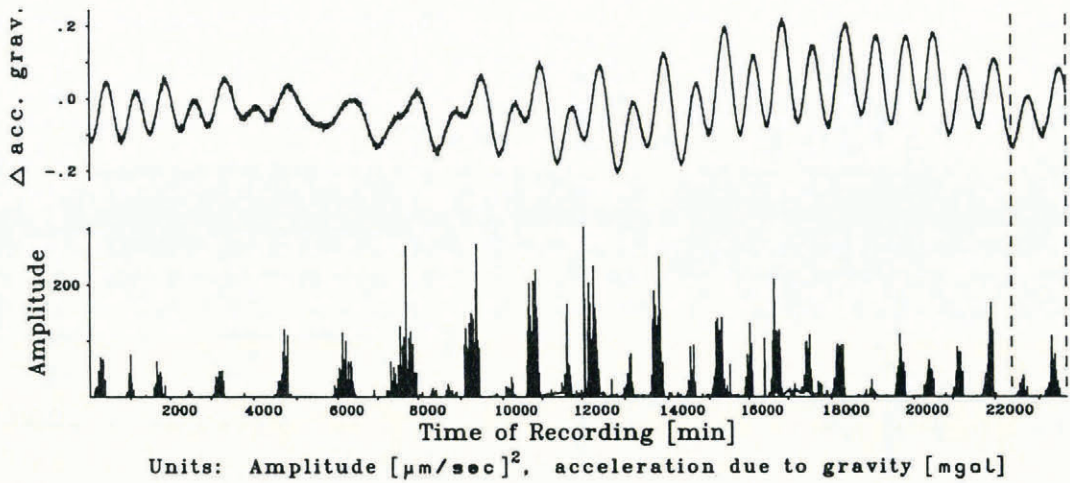


Fig. 6. Seismic activity in the ice-rumple area is mostly dependent on the tides. To show also that maximal seismic activity occurs at the beginning of low tides, the tidal values of this time are plotted at the top of this figure. Short segment of the recording on the top of the ice rumple. 1 gal = 1 cm/s².

The recording of the South Sandwich Islands earthquake on 28 July 1985 ($M_b = 4.8$) made it possible to connect Equation (10) with the Richter magnitude. For the icequakes, Equation (7) yields:

$$M = -2.437 + \log \frac{A}{T} + 1.989 \log R. \quad (11)$$

This leads to icequake magnitudes between -1.82 and +0.51.

TIDAL-DEPENDENT SEISMICITY OF THE ICE-RUMPLE AREA

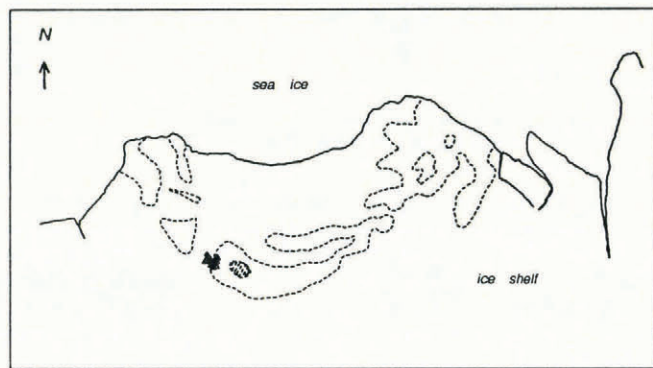
The seismicity of this area was not only recorded for 30 s after event detection but also during a 16.5 d interval with a sample rate of 78 values per second per station. The last experiment is to investigate the observed tidal-dependent seismicity.

The rate of seismicity (i.e. numbers of events per time unit) is represented by the 1 min mean values of the square of the amplitudes. The mean values of the seismic time series recorded at station 8 are presented in Figure 6. Because the recordings are proportional to velocity, these mean values are a measure of the seismic energy released.

Comparing the data series of the accelerations due to tides and the mean values of the square of the amplitudes (Fig. 6), it is evident that the highest seismic activity is recorded during the time between high tide and low tide. Moreover, comparing corresponding recordings from the other seismic stations, the beginning of an active period (i.e. time interval of extremely high seismicity) is dependent on the site of the seismic station; often the start of an active period is first recorded at the ice-rumple top station (station 8), followed by the stations to the south and later on by the stations to the north of the ice rumple. Such "time delays" can be in the range of up to 20–40 min. The locations of some epicentres of the icequakes, recorded at the beginning of such an active period, are shown in Figure 7. Calculation of the epicentres marked by "Δ" in Figure 7 was possible because of the three-component recordings of station "5–7", though these events were recorded only by this station. The hatched area in Figure 7 (around station 8) gives the possible sites of epicentres of events which are recorded only by this vertical component station. For the calculation of the distances to the hypocentres for these events,

$$R = v_p v_s \frac{t_s - t_p}{v_p - v_s} \quad (12)$$

with R as the distance between station 8 and the



----- Limits of the Ice Rumples
 Δ Epicentre

Fig. 7. Locations of epicentres of ice-rumple events, recorded at the beginning of an active seismic period of this area (see text). North is at the top.

hypocentre, t_p as the arrival time of the P-wave with wave-velocity v_p , and t_s as the arrival time of the S-wave with wave velocity v_s , was used. These events show extremely small maximum amplitudes ($<0.05 \mu\text{m/s}$).

At the high point of a seismically active period, the greatest seismic energy (1 min mean values) was recorded at stations "5–7" and 8. For example, the ratio of mean values at the maximum of the active period on 6 August is

$$\text{station 2} : \text{station 4} : \text{station 6} : \text{station 8} = 1.0 : 3.6 : 83.2 : 60.7. \quad (13)$$

Figure 8, which presents the section marked by the two dashed lines in Figure 6, shows clearly that these seismically very active periods are not characterized by continuous high activity but by short bursts of high activity (duration mostly 2–4 min), and intervals of relatively low activity, especially at the beginning and end of such a period. This suggests a kind of "grater effect" at the ice-rock boundary; because of high friction at this boundary, there seems to be a jerky vertical movement of the ice shelf in response to tides.

RESULTS: MODEL IDEAS

The seismic events recorded in the inlet and in the ice-rumple areas are based on different kinds of ice-dynamic processes in these areas; in the inlet area, they are caused by the separation of parts of the ice shelf

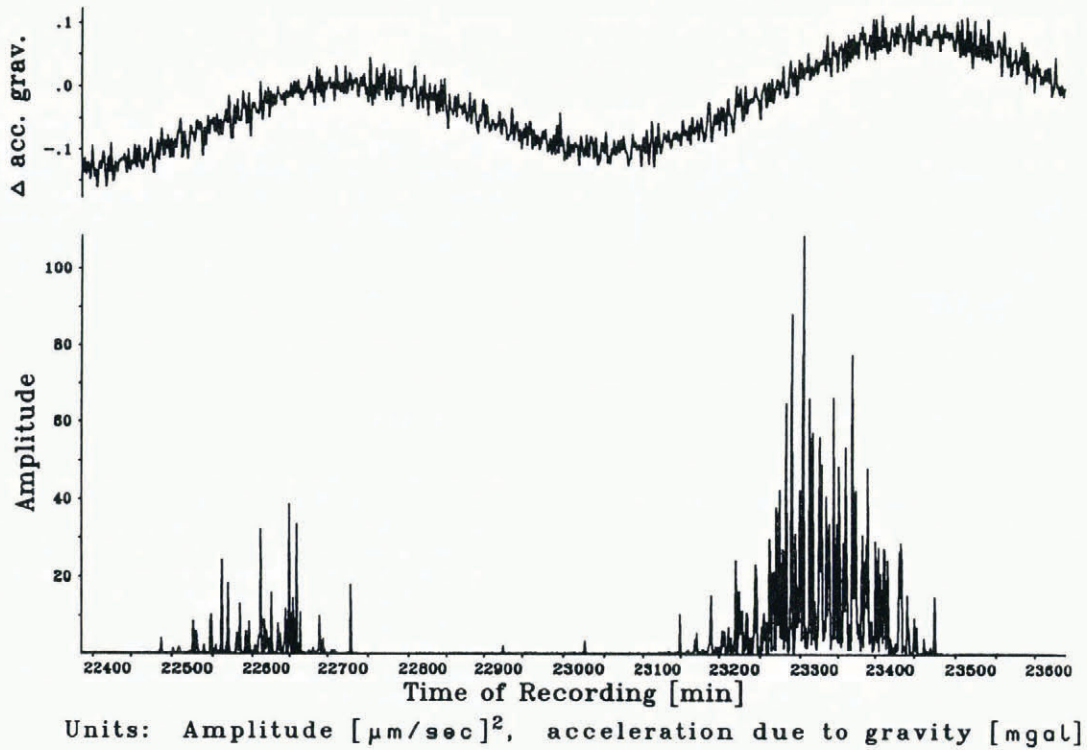


Fig. 8. Seismic activity in the ice-rumple area and its dependence on the tides. Plot of the marked section in Figure 6. The seismically very active periods are characterized by short bursts of high activity and intervals of low activity which implies a kind of "grater effect" at the ice-rock boundary. 1 gal = 1 cm/s².

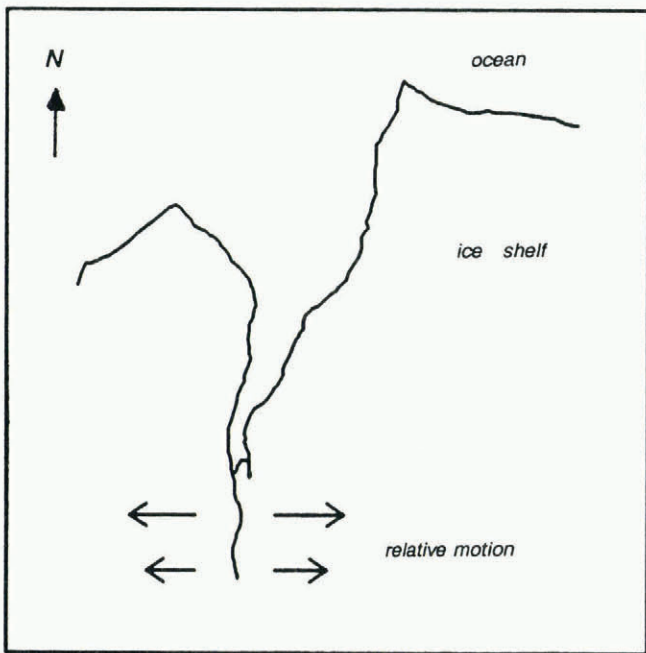


Fig. 9. In the inlet area, icequakes are caused because of the separation of parts of the ice shelf; the focal mechanism of these events is tensile fracture. No tidal dependency of the local seismicity was observed. Because of the tides, the whole of the inlet is raised in a uniform vertical movement.

(Fig. 9), and the focal mechanism of these events is tensile fracture. No tidal dependency of the local seismicity was observed; because of the tides, the whole of the inlet is raised in a uniform vertical motion in these areas.

Compared with the seismicity in the inlet area, extremely high seismic activity is observed in the

ice-rumple area. More than about 90% of this seismicity is dependent on tides; the most seismically active periods are during the period between high tide and low tide. During this time, up to 140 icequakes per minute were recorded at station 8. Because of the north-north-east directed flow of the ice, a relative motion of the ice at the ice rumple as shown in Figure 10a is to be expected, which is parallel or anti-parallel to the relative motion vector shown in Figure 10a, dependent respectively on situations. During the

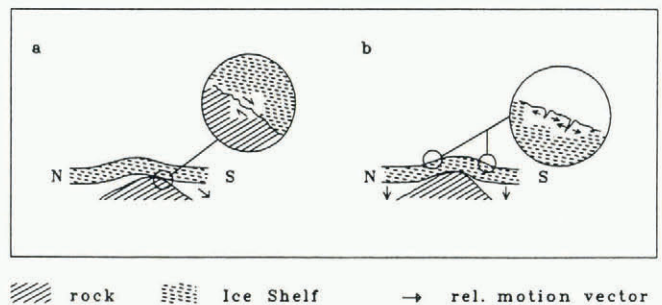
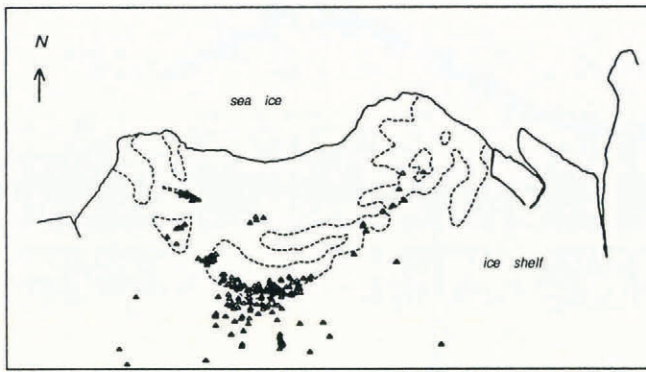


Fig. 10. See text. The relative motion of the ice plate at the beginning of low tide is shown in Figure 10a, respectively, by a right-down arrow and by right-left half-arrows for the process of rupture at the rock-ice boundary. Figure 10b represents the situation shortly before the end of low water.

time between high tide and low tide, this vector has a component which is directed anti-parallel to the flow-velocity vector; in the area south of this ice rumple we can expect a build-up of more stress in the ice in a relatively short period of time compared to the average for the area. Indeed, the highest seismic activity in this area is measured by those seismic stations situated in this part of the ice rumple (see Equation (8); stations 6 and 8; and Fig. 11). Because of the friction between the ice and the rock, the focal mechanism of the events caused by this process is a



----- Limits of the Ice Rumples
 ▲ Epicentre

Fig. 11. Locations of epicentres of ice-rumple events, recorded during an active seismic period.

shear mechanism; the first onset of the P-wave recorded by seismic station 8 (see Fig. 1), which was situated at the top of the ice rumple, indeed shows dilation, which is consistent with a shear mechanism. At almost low water, when the ice shelf is again in good contact with the rock beneath and the water level decreases further, we also record icequakes which are near the surface as shown in Figure 10b and whose focal mechanism is tensile fracture.

The focal mechanism of "single events", i.e. events which have not been recorded within such seismically very active time periods and with epicentres in the array area, is also tensile fracture. The events with hypocentres near the surface can be associated with the opening of crevasses.

ACKNOWLEDGEMENTS

I gratefully acknowledge Professor Dr G. Angenheister, Institut für Allgemeine und Angewandte Geophysik, München, for valuable discussions and contributions to this work. For placing various apparatus at my disposal, I am most grateful to Professor Dr H. Miller, Alfred-Wegener-Institut für Polar- und Meeresforschung, Bremerhaven, Professor Dr H. Soffel, München, and Professor Dr G. Angenheister. Thanks are also due to Dr G. Sherwood for reviewing the manuscript. Without the energetic help of some other members of the overwintering group, especially our station leader Dr H. Wortmann, these measurements would not have been possible. This work is supported by the Hanns-Seidel-Foundation, München.

REFERENCES

- Aki, K. and P. Richards. 1980. *Quantitative seismology*. San Francisco, CA, W.H. Freeman.
- Bath, M. 1981. Earthquake magnitude – recent research and current trends. *Earth Sci. Rev.*, 17, 315-398.
- Brodtscholl, A. Unpublished. Geophysik. Messungen während der Überwinterungskampagne 1983/84. Bremerhaven, Alfred-Wegener-Institut.
- Brune, H.N. 1970. Tectonic stress and the spectra of seismic shear waves from earthquakes. *J. Geophys. Res.*, 75(26), 4997-5009.
- Hoyer, M. Unpublished. Auswertung glaziologisch-geophysikalischer Messungen auf dem Ekström-Schelfeis. Westfälische Wilhelms-Universität Münster.
- Kobarg, W. and E. Lippmann. 1986. Gezeitenmessungen auf dem Ekström-Schelfeis, Antarktis. *Polarforschung*, 56(1/2), 1-21.
- Köhler, M. 1981. Das Verformungsverhalten des Ekström-Schelfeises in der Nähe der deutschen Antarktis-Forschungsstation "Georg von Neumayer". *Polarforschung*, 51(2), 113-127.

MS. received in revised form 20 October 1988